JOURNAL OF VIROLOGY, Sept. 2001, p. 7995–8007 Vol. 75, No. 17
0022-538X/01/$04.00+0 DOI: 10.1128/JVI.75.17.7995–8007.2001

Specific Interaction of a Novel Foamy Virus Env Leader Protein with the N-Terminal Gag Domain

THOMAS WILK,[1,2] VERENA GEISELHART,[3] MATTHIAS FRECH,[4] STEPHEN D. FULLER[1,2] ROLF M. FLÜGEL,[3] AND MARTIN LÖCHELT[3]*

Structural Biology Programme, European Molecular Biology Laboratory,[1] and Abteilung Retrovirale Genexpression, Forschungsschwerpunkt Angewandte Tumorvirologie, Deutsches Krebsforschungszentrum,[3] Heidelberg, and Merck KGaA, D-64293 Darmstadt,[4] Germany, and Division of Structural Biology, Wellcome Trust Centre for Human Genetics, University of Oxford, Oxford, United Kingdom[2]

Received 12 March 2001/Accepted 31 May 2001

Cryoelectron micrographs of purified human foamy virus (HFV) and feline foamy virus (FFV) particles revealed distinct radial arrangements of Gag proteins. The capsids were surrounded by an internal Gag layer that in turn was surrounded by, and separated from, the viral membrane. The width of this layer was about 8 nm for HFV and 3.8 nm for FFV. This difference in width is assumed to reflect the different sizes of the HFV and FFV MA domains: the HFV MA domain is about 130 residues longer than that of FFV. The distances between the MA layer and the edge of the capsid were identical in different particle classes. In contrast, only particles with a distended envelope displayed an invariant, close spacing between the MA layer and the Env membrane which was absent in the majority of particles. This indicates a specific interaction between MA and Env at an unknown step of morphogenesis. This observation was supported by surface plasmon resonance studies. The purified N-terminal domain of FFV Gag specifically interacted with synthetic peptides and a defined protein domain derived from the N-terminal Env leader protein. The specificity of this interaction was demonstrated by using peptides varying in the conserved Trp residues that are known to be required for HFV budding. The interaction with Gag required residues within the novel virion-associated FFV Env leader protein of about 16.5 kDa.

The genomes of spumaretroviruses (or foamy viruses [FV]) include the classical *gag, pro-pol*, and *env* genes that are the hallmark of the retrovirus family (9). Despite the familial relationship implied by their genome organization, FV differ from retroviruses such as oncoviruses or lentiviruses in basic aspects of replication and gene expression (30–32, 39, 53). The differences between FV and the more widely studied retroviruses, such as human immunodeficiency virus (HIV) or murine leukemia virus, provide an opportunity to identify the fundamental mechanisms of processes such as particle assembly and maturation.

The shared gene order of the FV genomes and those of other retroviruses allows the identification of common structural proteins. Unfortunately, this relationship does not extend to the structure and function of FV Gag proteins, since no obvious homologies are detectable between FV Gag and MA, CA, and NC domains of other retroviruses for which structures have been determined to high resolution (10, 43). Furthermore, the proteolytic processing of Gag that produces the familiar mature proteins in other retroviruses is unusual, incomplete, and/or delayed in FV (12, 23, 29, 37).

The available data indicate that the morphology and morphogenesis of FV are distinct from those of other retroviruses. FV Gag proteins preassemble to form in the cytoplasm spherical capsids that bud through cellular membranes (55). This process contrasts with what occurs with lentiviruses and C-type retroviruses that assemble their capsids at the site of budding but is similar to what occurs with B- and D-type retroviruses (40). Budding of human foamy virus (HFV) is strictly dependent upon the presence of Env proteins (4, 38), while budding of the other retroviruses occurs in the absence of Env. Recent results indicate that the Env leader protein (Elp) of HFV is the region that supports budding (D. Lindemann, personal communication). Electron microscopy (EM) of thin sections did not reveal the condensation of the ring-like capsids in FV particles after budding which is characteristic for the maturation of other retroviruses. Rearrangements of the FV capsids were rarely observed (34) or may not occur (14, 55). This lack of morphological maturation has been attributed to the incomplete processing of FV Gag proteins described above.

Cleavage of Gag in other retroviruses is believed to modulate its affinity for the membrane by altering the exposure of an amino-terminal acyl moiety and other motifs in MA (16, 57). The lack of complete proteolytic cleavage and the absence of basic sequence and myristylation motifs in MA that mediate membrane targeting in other retroviruses suggest that FV must bind to membranes by other mechanisms.

We combined cryoelectron microscopy (cEM) studies of HFV and feline foamy virus (FFV) particles with biosensor surface plasmon resonance (SPR) analyses of FV proteins to address the issues of Gag-membrane interaction. cEM has previously been used to demonstrate the lack of icosahedral symmetry and presence of local order in HIV and murine leukemia virus (20, 52), and it has revealed the radial arrangement of the Gag polyproteins and allowed the mapping of the

* Corresponding author. Mailing address: Abteilung Retrovirale Genexpression, Forschungsschwerpunkt Angewandte Tumorvirologie, Deutsches Krebsforschungszentrum, Im Neuenheimer Feld 242, 69120 Heidelberg, Germany. Phone: 49-6221-424853. Fax: 49-6221-424865. E-mail: m.loechelt@dkfz-heidelberg.de.

positions of individual domains in HIV type 1 Gag (48, 49). In FV particles, Gag proteins are radially arranged inside the virions, and lateral interactions of Gag domains result in the formation of the MA layer and the FV capsid shell. An intimate association of the Gag MA layer and the viral membrane was detected in 20% of FFV particles. SPR technology demonstrated a direct and specific physical interaction of the FFV Elp with the N terminus of Gag. This result and the detection of the 16.5-kDa FFV Elp in released virions suggest a putative transient interaction of the MA layer and Elp during particle morphogenesis of FV.

MATERIALS AND METHODS

Cells and virus. Crandell feline kidney (CRFK) and HEL299 cells were grown as reported previously (50). FFV isolate FUV and the prototypic HFV were propagated as described previously (33, 50).

Purification of released FV particles. Cell culture supernatants from HFV-infected HEL299 or FFV-infected CRFK cells were harvested 4 to 6 days after infection, when the infected cells displayed strong virus-induced cytopathic effects. Cell culture supernatants were cleared by centrifugation at 400 × *g* for 7 min and then at 3,000 × *g* for 30 min (46). Supernatants were filtered through 440-nm-pore-size filters and centrifuged through 5 ml of 20% (wt/vol) sucrose in TEN (150 mM NaCl, 10 mM Tris/HCl [pH 8.0], 1 mM EDTA) for 2 h at 24,000 rpm in an SW27 rotor (Beckman, Munich, Germany). The resulting pellet was gently resuspended in phosphate-buffered saline. For further purification, the enriched particles were separated on sucrose gradients (48) or banded in a preformed 10 to 32% iodixanol (Optiprep; Nycomed Pharma, Oslo, Norway) gradient in TEN run for 16 h at 32,000 rpm in an SW41 rotor (Beckman) (3).

cEM, image analysis, and contrast transfer function correction. cEM was performed as described previously using a Philips CM200FEG operated at 200 kV at a magnification of ×38,000 (20, 49). The images were digitized on a Zeiss (Oberkochen, Germany) SCAI scanner at a step size of 14 μm. The measurements shown in Fig. 4 were performed using the SPIDER image analysis program (15). The particle diameter was measured from the outer leaflet of the membrane and thus excludes the contribution of the projection domains of the viral glycoproteins.

The defocus of the micrograph was determined from the positions of the local minima in a radially averaged power spectrum. Contrast transfer function (13) correction was performed by division of the transform of the image with the appropriate phase contrast transfer function as described previously (11).

Expression and purification of recombinant FFV Gag and Elp. FFV Gag residues 1 to 154 were bacterially expressed in the pET16b (Novagen, Madison, Wis.) vector as described previously (5). The FFV Gag residues 1 to 154 were flanked at the N terminus by the vector-encoded His tag and 16 unrelated residues at the C terminus. Induced *Escherichia coli* BL21 cells were lysed in IMAC buffer in the absence of urea or other denaturing agents by sonification (5). The soluble recombinant FFV Gag 1 to 154 was purified to more than 95% homogeneity using Ni affinity chromatography, dialyzed against phosphate-buffered saline, and stored at −70°C before use. Elp residues 1 to 65 were amplified by PCR with primers 5′-GCTCATGATGGAACAAGAACATGTG-3′ (the introduced *Bsp*HI site is underlined) and 5′-GGAATTCTCATCTAGTAGAAG TAGCACA-3′ (the introduced *Eco*RI site is underlined) as described previously (55). The amplicon was digested with *Bsp*HI and *Eco*RI and inserted into the *Nco*I- and *Eco*RI-digested vector pET32c (Novagen). The resulting thioredoxin-Elp fusion protein of 25 kDa and the pET32c-derived thioredoxin control protein were purified to about 90% homogeneity under nondenaturing conditions by His tag affinity chromatography as described above.

Immunoblotting and induction of an Elp-specific antiserum. Immunoblotting of proteins separated on denaturing gels and detection of specifically bound antibodies by enhanced chemiluminescence and diamino-benzidine staining were done as described previously (1, 37). Synthesis of authentic and mutant Elp-derived peptides was as recently described (37). A synthetic peptide encompassing the authentic FFV Env residues 1 to 30 was directly used for immunization of guinea pigs by Eurogentec, Seraing, Belgium. The FFV MA and Env surface (SU) antisera and cat antiserum 8014 were as described previously (1, 5, 56).

Binding analysis by SPR. Protein interactions were identified and characterized by SPR technology using the BIAcore 3000 instrument (BIAcore, Freiburg, Germany) and methodology (26, 27). Coupling reagents were used according to protocols developed by the supplier.

TABLE 1. Structural features of HFV and FFV particles[a]

Virus	Diam in nm of enveloped particles (*n*)	Diam in nm of capsids in particles (*n*)	Length in nm of the spike glycoprotein (*n*)	Width in nm of the MA layer (*n*)
HFV	106.9 ± 8.3 (48)	61.2 ± 5.9 (57)	15.6 ± 2.1 (83)	8.2 ± 0.9 (62)
FFV	109.1 ± 11.2 (55)	63.5 ± 7.8 (90)	14.0 ± 1.9 (103)	3.8 ± 0.7 (65)

[a] Values are means ± standard deviations.

Coupling to the CM5 sensor chip was done via activated carboxylate groups to amine groups of the recombinant FFV Gag 1 to 154 protein (Gag 1–154) which was purified to homogeneity as described. Analysis of the pH dependence of protein coupling (pH scouting) and the coupling chemistry were performed under standard conditions (26, 27). The purified FFV Gag 1–154 protein was diluted into 10 mM acetate buffer (pH 4.5) to a final concentration of 20 μg/ml for coupling to the sensor chip. After the coupling chemistry, about 1,500 relative response units as base signal were immobilized on the sensor chip and gave a stable signal. The Elp peptides and the recombinant Elp protein were dissolved in 10 mM HEPES (pH 7.4)–150 mM NaCl–3 mM EDTA–0.005% Tween 20 (HBS buffer) for binding analyses. Binding experiments were performed in HBS buffer at 25°C. For each protein analyzed, a single chip was employed and measurements were done twice and in duplicate. Peptide concentrations were varied from 0.78 to 50 μg/ml, corresponding to 2×10^{-7} to 1.33×10^{-5} M. Reverse experiments in which the recombinant Elp protein and Elp-derived peptides were coupled to sensor chips and probed with recombinant FFV Gag1-154 were performed under similar conditions. SPR data analysis was done with the integrated BIAcore 3000 software.

A bacterially expressed HIV-1 MA protein encompassing residues 1 to 132 was purified by ion-exchange chromatography and gel filtration and served as control (T. Wilk, unpublished data). An antiserum directed against HIV-1 MA was kindly provided by H.-G. Kräusslich, Heidelberg, Germany.

RESULTS

cEM of released enveloped and nonenveloped HFV particles. HFV particles released into the supernatant of infected cells were harvested and concentrated by sedimentation through sucrose. This protocol isolated enveloped HFV particles that were heterogeneous in size and shape together with some cell debris. The virions ranged in size between 55 and 250 nm and displayed a mean membrane-included diameter of 106.9 ± 8.3 nm (mean ± standard deviation) ($n = 48$) (Table 1). The particles were covered with spikes 15.6 ± 2.1 nm long ($n = 83$) that formed clusters on the virion surfaces (46). Capsid structures with diameters of ≈60 nm were present within the enveloped particles. The enveloped capsids were neither completely spherical nor regular but appeared angular without any apparent symmetry.

Spherical, nonenveloped particles with diameters of ≈60 nm were also present in supernatants of HFV-infected cells (data not shown). These spherical particles resembled the capsids observed within the enveloped virions and may represent preassembled intracellular capsids that had been released by cell lysis (4, 14, 29, 34, 55).

Organization of HFV particles. HFV particles purified by an additional sucrose centrifugation step (see Materials and Methods) banded at a density of approximately 1.16 g/ml, similar to that described for other retroviruses (45). Spherical HFV particles with tightly packed spikes (Fig. 1B) inserted into the viral membrane (Fig. 1A) predominated in this purified material (for a schematic presentation, see Fig. 1C and 2D). The projecting region of the spike displayed a layered appearance that was most apparent within the spike clusters, suggesting that the structural features of the Env complexes were

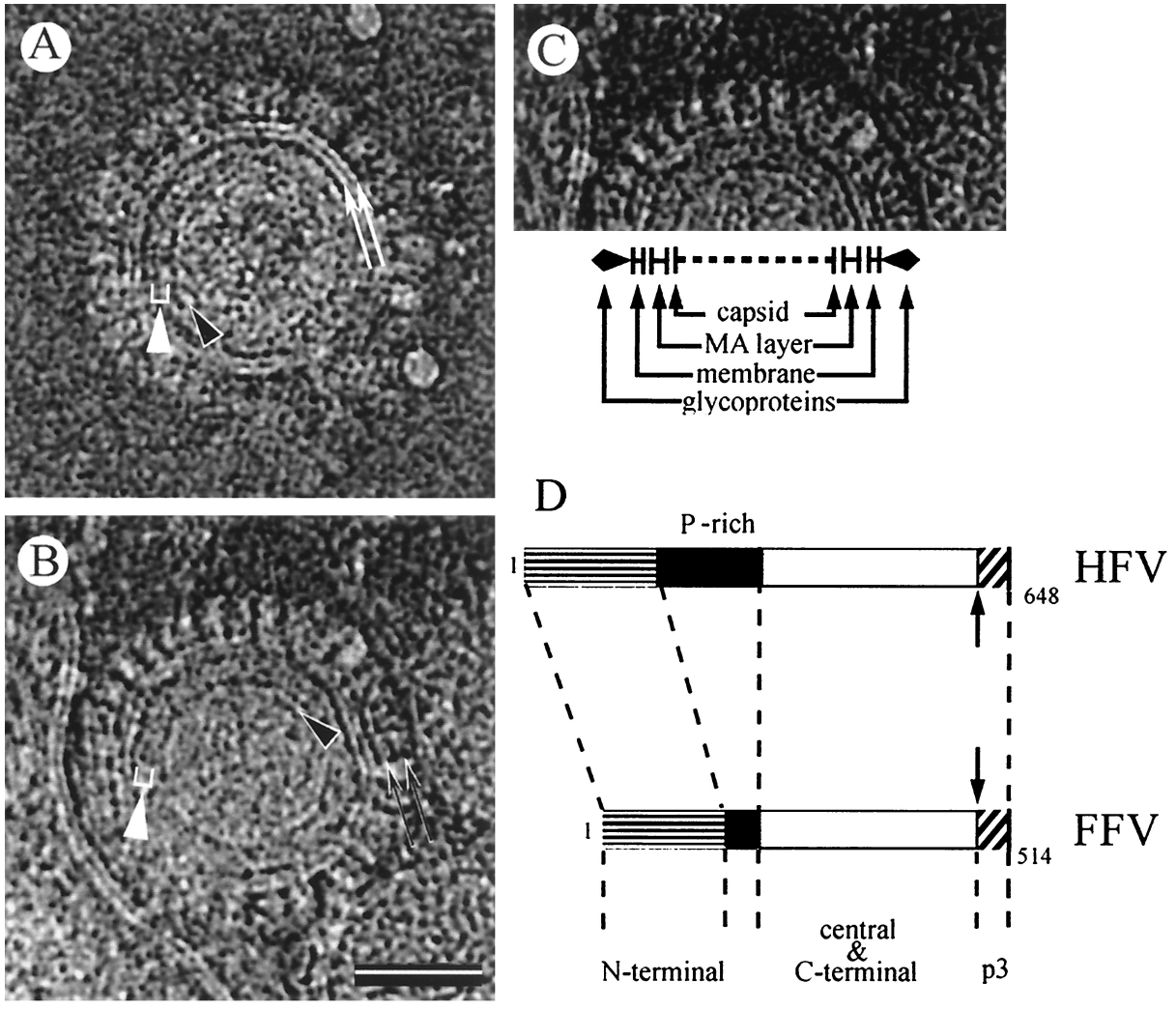

FIG. 1. Ultrastructure of released HFV particles (A to C) and schematic alignment of HFV and FFV Gag proteins (D). cEM of HFV reveals closely packed envelope proteins with distinct layers of density within the glycoproteins (pair of black arrows in B) covering the surface of the budded virion. A separation between the viral membrane (pair of white arrows) and the broad MA layer (white bracket and white arrowhead) is clearly visible and characteristic for budded FV particles. The MA layer width of about 8 nm is characteristic for HFV. The prominent margin of the angular HFV capsid is marked with a black arrowhead. The capsid in panel A has a central position in contrast to the off-center position of the capsid shown in panel B. The scale bar in panel B represents 50 nm. (C) Schematic presentation of structural features of HFV particles analyzed by cEM. (D) Schematic alignment of HFV and FFV Gag proteins. The presence of the C-terminal p3 cleavage site (arrow), the p3 protein, and the N-terminal, Pro-rich (P-rich), and central and C-terminal subdomains of FV Gag proteins is shown. For details, see the text.

laterally aligned in the clusters (Fig. 1B). A fraction of the particles displayed a distorted membrane and an asymmetric distribution of Env proteins and even contained two capsids as discussed below in detail for FFV.

cEM revealed that the majority of HFV particles contained one angular, isometric capsid (Fig. 1A, black arrowhead pointing to the edge of the capsid) that was centered in the particle. Standard common line methods (2, 13a, 18, 19) provided no evidence of icosahedral symmetry in the isometric particles of the preparation. In some HFV particles, the angular capsids were displaced toward the periphery (Fig. 1B).

HFV capsids were surrounded by a protein layer 8.2 ± 0.9 nm wide which maintained a relatively fixed distance to the body of the capsid (Fig. 1). We will refer hereafter to this protein layer as the MA layer in analogy to the region which separates the capsid from the membrane in immature retroviruses (45, 49). In order to determine whether this MA layer is common to other FV, virus particles from the distantly related FFV were analyzed by cEM.

The width of the MA layer is characteristic for different FV. Enveloped FFV particles measured 109.1 ± 11.2 nm (n = 55) in diameter and banded at a density of 1.16 g/ml. Surface staining of isolated FFV particles showed tightly packed glycoprotein complexes (data not shown) similar to those described previously for HFV (46). cEM analysis showed the spikes as projections 14 ± 2 nm (n = 103) long, with strong lateral interactions resulting in the formation of clusters as also observed in HFV. FFV particles contained an angular capsid of 63.5 ± 7.8 nm (n = 90) (Table 1 and Fig. 2D). Capsids were always separated from the viral membrane by a protein layer

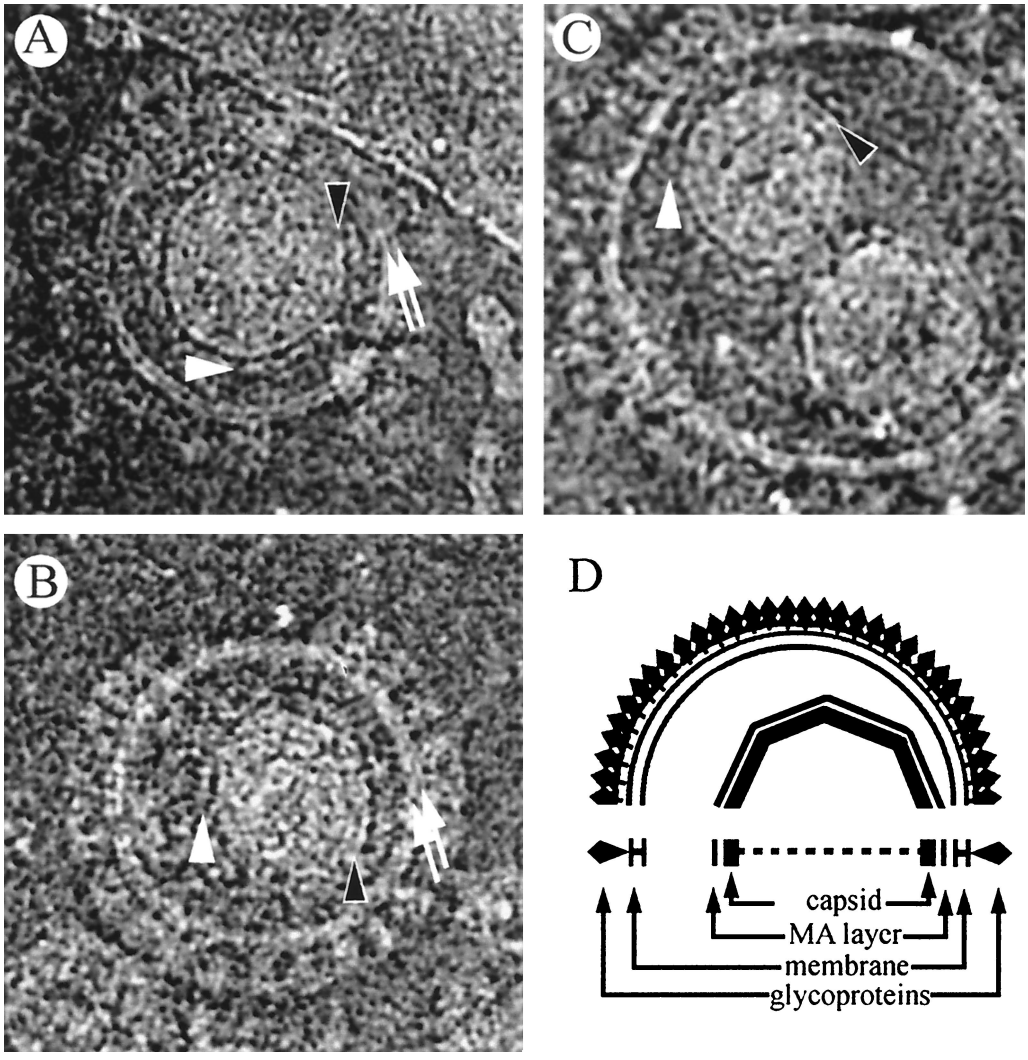

FIG. 2. Ultrastructure of released FFV particles (A to C) and schematic diagram of FFV particles (D). The MA layer (white arrowheads) follows the shape of the capsids in particles with central (A) and off-center (B) capsids as schematically shown in panel D. Many particles in the population show the internal angular capsid (the edge of the capsid is marked by black arrowheads) displaced from the center of the particle (B). Views in which the capsid appeared to be almost in the center of the particle were also observed (A). Occasionally, two capsids were surrounded by an almost perfect spherical viral membrane (pair of white arrows), resulting in particles with a greater diameter (B and C).

resembling the MA layer of HFV (Fig. 1 and 2). The thickness of the MA layer between the capsid and the viral envelope was the only consistent difference between HFV and FFV particles. Close examination of a large number of virions revealed an MA layer consistently thinner in FFV (3.8 ± 0.7 nm [$n = 65$]) than in HFV (8.2 ± 0.9 nm [$n = 62$]) (Table 1). This difference in the sizes of the MA layers may correspond to 130 additional residues in the N-terminal region of HFV compared with FFV (Fig. 1D) (42, 50).

Localization of the MA layer in distinct classes of FFV particles. In 25% of the FFV particles analyzed, the isometric, angular capsid was positioned in the center of the particle (Fig. 2A). The MA layer appeared to follow the edge of the capsid, resulting in a variable distance between the MA layer and the viral membrane. That the FFV MA layer followed the shape of the capsid and was not associated with the viral membrane was more obvious when the capsid was displaced from the center of the particle (Fig. 2B). Such particles with off-center capsids represented 50% of the virus population. The ratio of central to off-center capsid locations suggests that they arise from the same particle morphology (i.e., an off-center capsid) viewed from different directions in cEM. About 5% of the particles contained two displaced capsids. In these particles, the MA layer maintained a relatively fixed distance to the body of the capsid with no obvious physical interaction with the viral membrane (Fig. 2C). In both particle types described above, the MA layer appeared to be separated from the viral membrane but was consistently localized next to the angular viral capsid as schematically shown in Fig 2D.

About 20% of the FFV particles displayed a distended morphology: their envelopes were distended and incompletely closed, and the particles were thus composed of a spherical portion and a protruding tail (Fig. 3). These particles with distended morphology displayed strong evidence for an inter-

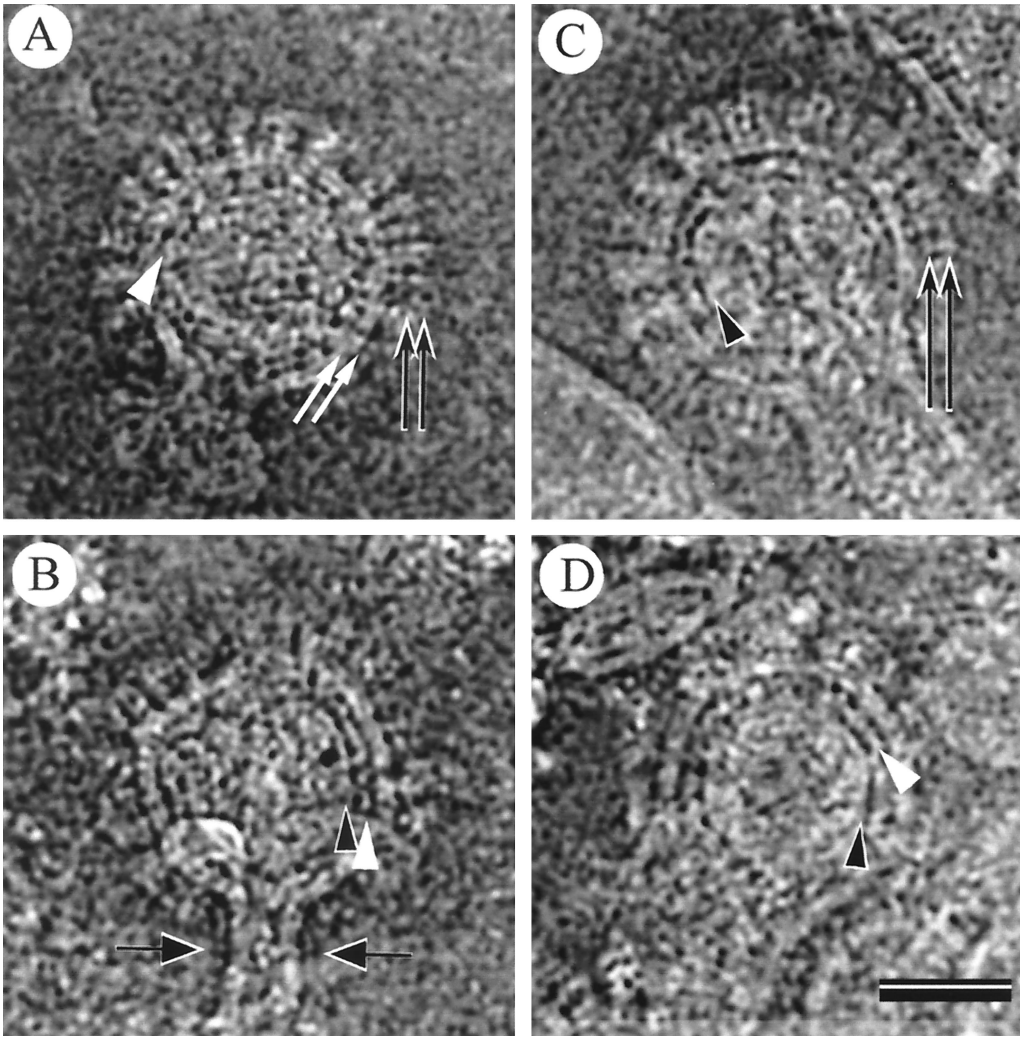

FIG. 3. Features of FFV particles with a distended morphology. Particles with a distended morphology (A to D) show tight interaction of the MA layer (white arrowheads) with the viral membrane (pair of white arrows). The two opposed arrows mark the stalk of cellular membrane which is still attached to the particle (B). The pairs of black arrows mark spike proteins, and the black arrowheads point to the margin of the capsid. The scale bar in panel D represents 50 nm.

action of the MA layer with the viral membrane. The MA layer was located significantly closer to the viral membrane than in the FFV particles with a central or off-center capsid described above (Table 2). In addition, the similar periodicities of the projections on the particle surface and the inner structural components suggest an interaction between the Gag proteins and components of the viral membrane. Particles with a corresponding morphology were also found in HFV (not shown).

We measured the distances between the MA layer and the viral membrane and between the MA layer and the capsid layer to define the different morphology of the distended particles. The spacing between the membrane and the MA layer and between the MA layer and the capsid was measured at 1-nm intervals along the circumference of the MA layer in different types of particles. The measurements of individual particles demonstrate the constant distance between the capsid and the MA layer over several microns of arc (Fig. 4A). The spacing was unchanged between FFV particles that displayed

TABLE 2. Relative abundance of different FFV particle morphologies and distances between the MA layer and the capsid and between the MA layer and the viral membrane in defined FFV particle types

FFV particle morphology	Relative abundance in FFV particles (%)	Distance (nm) between MA layer and capsid (*n*)	Distance (nm) between MA layer and viral membrane (*n*)
Central capsid	25	5.5 ± 1.0 (85)	8.8 ± 1.4 (85)
Off-center capsid	50	5.6 ± 0.9 (133)	18.3 ± 11.4 (133)
Distended particles	20	5.9 ± 0.7 (100)	6.0 ± 0.8 (83)

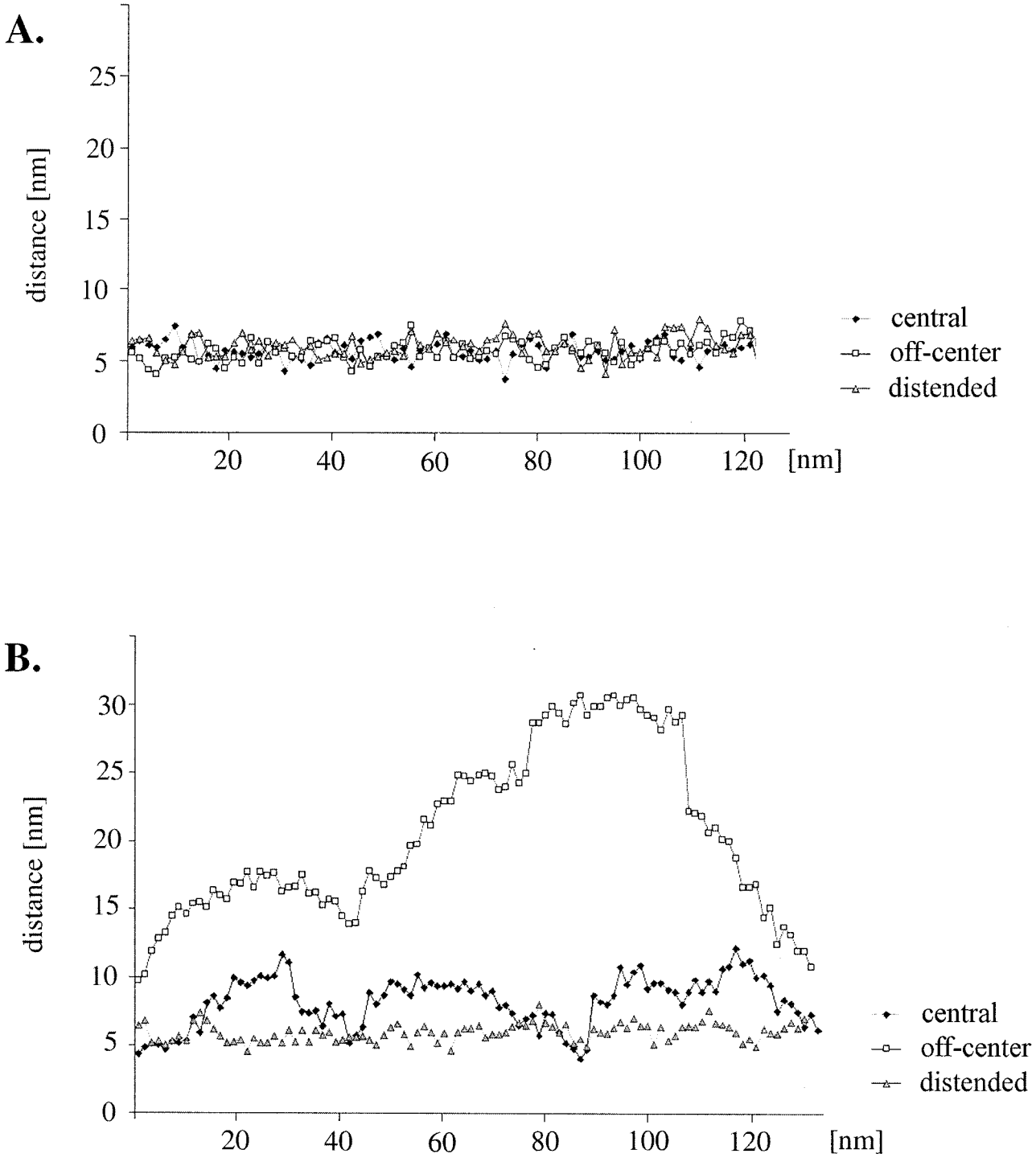

FIG. 4. Relative localization of the MA layer in FFV particles. Arrangement of the MA layer in FFV particles with central capsids (diamonds), off-center capsids (squares), and distended morphology (triangles). The plots show the distribution of distances between the MA layer and the edge of the capsid structure (A) and between the MA layer and the inner leaflet of the viral membrane (B). The distances in nanometers are plotted against the position of the measurement on the circumference of the MA layer and were measured at 1-nm intervals. A typical result is shown for each particle type. No significant difference is seen between the mean distances from the capsid to the MA layer of the three particle types (A). In contrast, only the distended FFV particles showed a constant and close juxtaposition between the MA layer and the membrane, with a distance of 6.0 ± 0.8 nm (mean ± standard deviation) (n = 83) (B). The mean distances from the membrane to the MA layer were 8.8 ± 1.4 nm (n = 85) for central capsids and 18.3 ± 11.4 nm (n = 133) for off-center capsids.

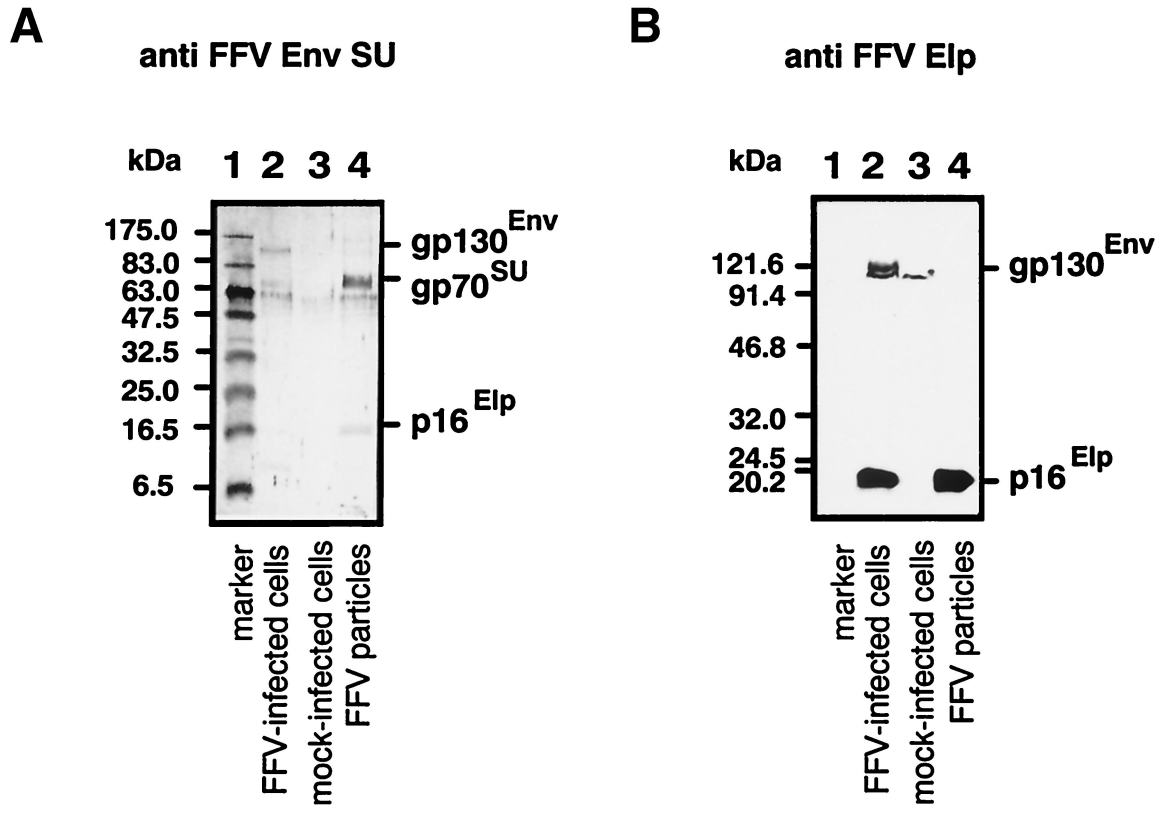

FIG. 5. Detection of FFV Elp in released FFV particles and FFV-infected cells. FFV particles were enriched from the cell culture supernatant from FFV-infected CRFK cells by centrifugation through sucrose as described in Materials and Methods, lysed, separated on a denaturing gel, and analyzed by immunoblotting (lanes 4). In parallel, proteins from FFV-infected (lanes 2) and mock-infected CRFK cells (lanes 3) were analyzed. The blots were reacted with the FFV SU antiserum (A) (56) and the FFV Elp antiserum (B) and specific proteins were detected by diaminobenzidine staining (A) and enhanced chemiluminescence (B). The positions of Elp, Env-SU, and the $gp130^{Env}$ precursor are marked. Two different prestained molecular mass markers were used in lanes 1. The gel in panel A contained 16% polyacrylamide, and that in panel B contained 14% polyacrylamide.

central capsids, off-center capsids, or the distended morphology (Fig. 4A). In contrast, only particles with the distended morphology maintained a constant distance between the MA layer and the viral membrane (Fig. 4B). The distance differed by up to 100% for particles with central capsids and by up to 300% for the off-center ones. The average values of these measurements using six different particles for each of the different virus morphologies are given in Table 2: the MA layer is very closely opposed to the viral membrane in distended forms, while both structures are significantly further separated from each other in particles with central and off-center capsids. While the interaction between the membrane and the MA layer is evident only in distended particles, the constant spacing between the MA layer and the capsid is maintained in each of the different particles, suggesting a tight and invariant link between the subunits of the MA layer and the viral capsid.

The FFV Elp is virus associated. Recent results demonstrate that the N terminus of HFV Env is required for particle budding and that this domain is cleaved off as a protein of about 148 residues by an unknown protease (D. Lindemann, personal communication). We analyzed whether a corresponding Elp is present in FFV, since this domain may be responsible for the Gag-envelope interaction seen in cEM of distended FFV particles. FFV particles enriched by centrifugation through sucrose and FFV antigen from infected CRFK cells were subjected to immunoblotting using the FFV Env SU antiserum directed against Env residues 101 to 402 and the FFV Elp serum directed exclusively against Env residues 1 to 30 (Fig. 5). The Elp antiserum detected exclusively FFV proteins of about 16.5 kDa in virion-associated antigens, which corresponds in size to the expected FFV Elp protein (Fig. 5B, lane 4). In extracts from FFV-infected cells, the Elp antiserum specifically detected the unprocessed Env precursor of 130 kDa and the 16.5-kDa Elp (Fig. 5B, lane 2) besides an unspecific band also present in mock-infected cells (lane 3). The FFV Env SU serum detected the 16.5-kDa Elp and the 70-kDa Env SU bands in enriched FFV virions (Fig. 5A, lane 4). At the antigen concentration used, the Env SU serum did not allow detection of the FFV Elp protein in FFV-infected cells (lane 2) whereas the Env precursor and the Env SU proteins were recognized in addition to a few weak and unspecific bands.

We then enriched FFV particles by centrifugation through 20% sucrose and subsequently analyzed them by sedimentation into a preformed iodixanol gradient. Regular aliquots of the fractionated gradient were analyzed by immunoblotting using the FFV-specific cat antiserum 8014 (1) and the FFV Elp

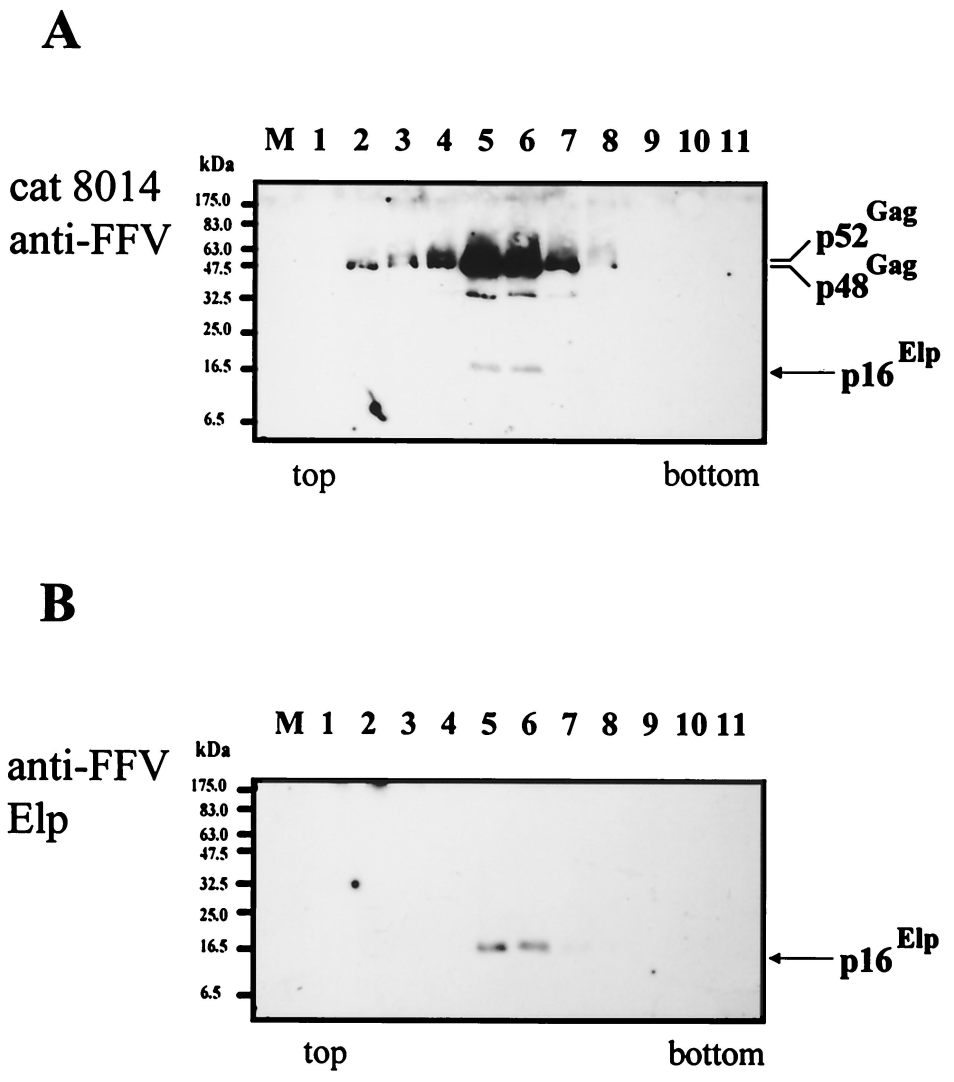

FIG. 6. Cosedimentation of FFV Elp with FFV particles. FFV particles enriched by centrifugation through 20% sucrose were analyzed on preformed 10 to 32% iodixanol gradients as described in Materials and Methods. Regular aliquots of the gradient fractions (as indicated) were directly analyzed by immunoblotting using the FFV-specific cat antiserum 8014 (A) and the FFV Elp antiserum (B). Proteins were detected by enhanced chemiluminescence. The positions of the p52 and p48 Gag and the FFV Elp proteins are marked. In lanes M, prestained molecular mass markers were separated in parallel.

antiserum (Fig. 6). The cat antiserum detected a peak concentration of FFV p52 and p48 Gag proteins in fractions 5 and 6 corresponding to a density of about 1.12 g/ml, similar to that reported for HFV particles (3). The 16.5-kDa Elp protein copurified into the same gradient fractions as seen with both antisera used (Fig. 6).

Preliminary studies using the bacterial protease subtilisin to digest proteins which copurify with virions or which are located on the surfaces of particles indicate that Elp is an integral component of FFV particles: the N-terminal half of Elp is subtilisin resistant, since this part of Elp is located inside the virion and thus not accessible to the protease (data not shown). These data demonstrate that the mature 16.5-kDa Elp protein is present in FFV virions. The Elp domain is not part of the mature virion-associated Env SU, whereas it is initially part of the unprocessed Env precursor in infected cells. Importantly, the N terminus of Elp is located inside the FFV particle.

Specific interaction of the N-terminal domains of FFV Gag and Elp determined by SPR. The close association between the MA layer and Env-bearing membrane regions described above for distended FFV particles may reflect a specific interaction between defined regions in Gag and Env. We used SPR to identify and characterize putative interactions between a portion of the N-terminal FFV Elp and the N-terminal region of the Gag polyprotein.

A bacterially expressed and purified recombinant N-terminal FFV Gag protein (residues 1 to 154) was immobilized on the sensor surface and probed with synthetic peptides comprising the N-terminal 30 residues of Env. At a peptide concentration of 50 μg/ml, this assay demonstrated specific binding of

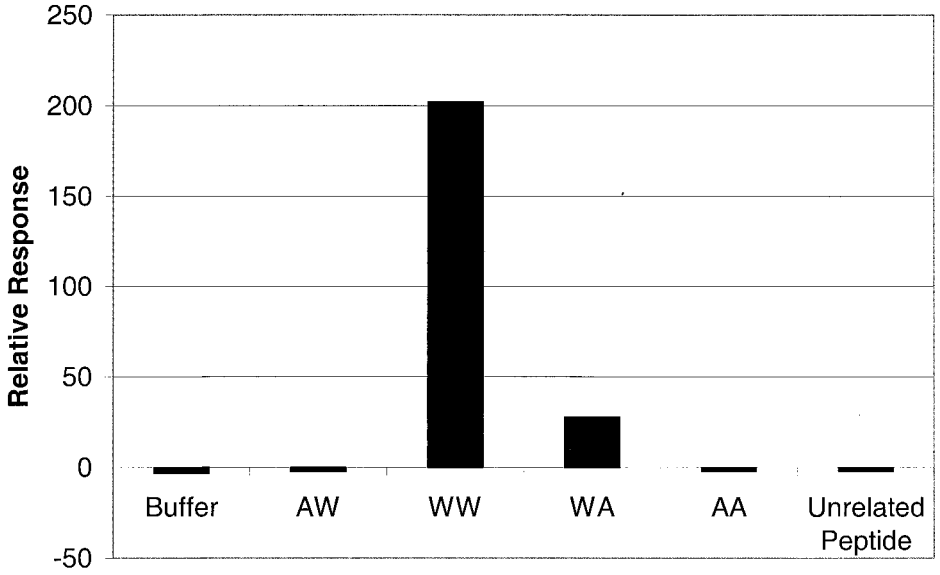

FIG. 7. Interaction of FFV Elp-derived peptides with FFV Gag 1–154. SPR analysis of the binding of FFV Elp-derived peptides to the recombinant N-terminal FFV Gag 1–154 domain bound to the sensor surface. Each peptide solution (50 μg/ml) was passed over the FFV Gag sensor surface at a flow rate of 10 μl/min for 3 min. The peptide representing the wt FFV (Elp residues 1 to 30) is designated WW, AW represents the single W12A, WA represents the W15A exchange, and both Trp residues have been replaced by Ala in peptide AA. A human collagen-derived peptide (unrelated peptide) served as an additional control. The signals for binding were automatically recorded after the binding reaction reached equilibrium and are presented as relative response units.

the wild-type (wt) peptide WW (Fig. 7). Elp peptides with alanine substitutions for either the first Trp (W12A) or both Trps (W12A, W15A) (peptides AW and AA, respectively) did not bind Gag 1–154 at the concentration of 50 μg/ml. Substitution of Ala for the second Trp (peptide WA) reduced binding to 14% of that obtained with the authentic FFV Elp peptide. No interaction was detected with an unrelated peptide derived from human collagen (Fig. 7).

Kinetic analyses of the interaction of recombinant FFV Gag with increasing concentrations of the wt Elp-derived peptide WW showed a clear dose dependence. The rapid association and dissociation of the peptide indicate a specific but relatively low affinity interaction (Fig. 8A). The half-life for the dissociation was estimated to be less than 5 s. Assuming a direct and hyperbolic function for the Elp peptide-MA interaction (26, 27), a dissociation constant of 1.52×10^{-5} M for the wt WW Elp peptide was calculated. Comparable dissociation constants and rapid on and off rates have been reported for the interaction of major histocompatibility complex proteins with defined peptide ligands (25, 41). Corresponding dissociation constants could not be determined for the mutant peptides by SPR, since their binding was significantly weaker or even absent (Fig. 7). The recombinant FFV MA protein used was accessible for molecular interactions, since the corresponding antiserum directed against this FFV Gag domain yielded a strong and specific interaction (Fig. 8B). The association of the MA antiserum with the corresponding membrane-bound MA protein was dose and time dependent, with a relatively stable binding signal over several minutes of measurement, indicating that the binding was strong and specific (Fig. 8B).

In reverse experiments, the authentic WW and the mutant Elp-derived peptides were bound to the sensor surface and probed with the purified recombinant FFV Gag 1–154 protein (data not shown). In full agreement with the data presented above, FFV Gag 1–154 bound to the authentic wt and, with a significantly lower affinity, to the WA Elp-derived peptides. Binding to the other mutant peptides was not observed.

In order to further substantiate the Gag-Elp interaction, Elp residues 1 to 65, which most probably correspond to the complete cytoplasmic domain of Elp, were expressed as a thioredoxin-Elp fusion protein in *E. coli*, purified, and analyzed for interaction with FFV Gag 1–154. As anticipated, the thioredoxin-Elp fusion protein exhibited a significantly stronger binding to MA than did the Elp WW peptide (Fig. 8C). Most importantly, the off rate was significantly slower, with a half-life of about 7 min, indicative of a stable Gag-Elp interaction. The thioredoxin protein lacking the Elp domain did not show specific binding to the immobilized FFV Gag 1–154, confirming the specificity of the Elp-Gag interaction described above (data not shown).

To further confirm the specificity of the FFV Gag-Elp interaction, the MA protein of HIV was bound to the sensor surface and probed with the wt and mutant Elp peptides. In these control experiments, no evidence for an interaction of FFV wt and mutant Elp peptides with the unrelated HIV MA protein was obtained, whereas a monospecific antiserum directed against recombinant HIV MA showed a strong and specific interaction (data not shown).

DISCUSSION

We have used cEM of FFV and HFV to address the relationship of FV structure to that of better characterized retroviruses such as B, C, and D types and lentiviruses. FV share the heterogeneous size of released retroviral particles, the lack of icosahedral symmetry, and the radial arrangement of defined

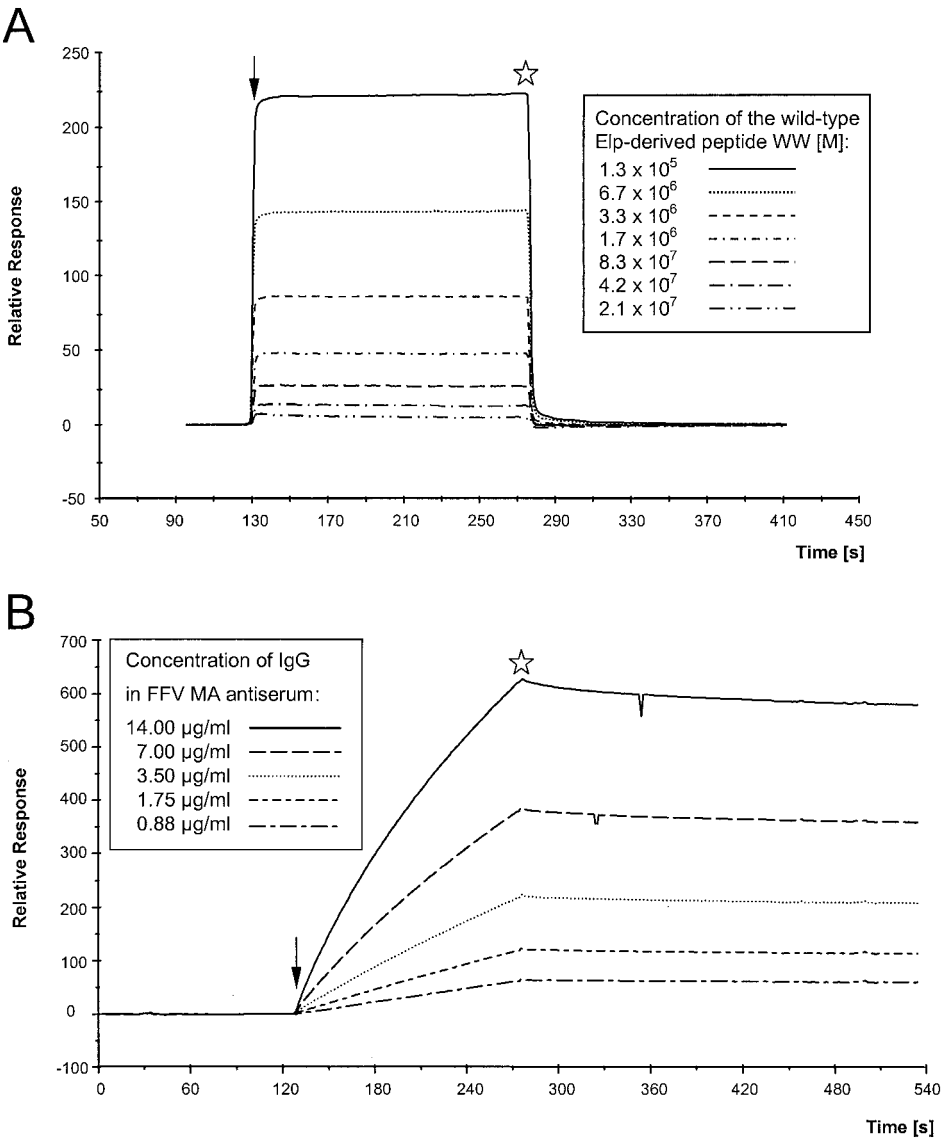

FIG. 8. (A) Kinetic analyses of the interaction of the authentic Elp-derived peptide with FFV Gag 1–154 coupled to the CM5 sensor. The peptide WW was passed over the sensor chip at a flow rate of 10 μl/min for 2.5 min at concentrations ranging from 2.08×10^{-7} to 1.33×10^{-5} M as shown in the inset. The fast associations and dissociations are graphically expressed as relative response over time in minutes. Regeneration of the sensor surface was complete and achieved by changing to HBS buffer. Arrow, start of the binding reaction; asterisk, beginning of the washing with HBS buffer. (B) Kinetic analyses of the interaction of the FFV MA antiserum with FFV Gag 1–154 coupled to the CM5 sensor. Defined dilutions of the FFV MA antisera ranging from 1:500 to 1:8,000 were passed over the sensor chip at a flow rate of 10 μl/min for 2.5 min corresponding to immunoglobulin G concentrations from 14 to 0.88 μg/ml as shown in the inset. The slow association of the polyclonal antiserum at concentrations reaching saturation and the very low dissociation of the bound antibodies are graphically expressed as relative response over time in minutes. (C) Kinetic analyses of the interaction of the FFV Gag 1–154 protein coupled to the CM5 sensor with the purified thioredoxin-Elp 1–65 fusion protein. Defined concentrations of the recombinant thioredoxin-Elp 1–65 fusion protein ranging from 62 to 15.5 μg/ml were passed over the sensor chip at a flow of 15 μl/min for 3 min. The slow and specific association of the thioredoxin-Elp 1–65 and the slow dissociation of the bound Elp protein are graphically expressed as relative response over time in minutes. The thioredoxin protein without the FFV Elp domain did not show any specific binding. Arrow, start of the binding reaction; asterisk, beginning of the washing with HBS buffer.

Gag domains with the other retroviruses that have been examined (20, 47, 49, 52).

Comparative cEM of HFV and FFV revealed the FV MA layer, a novel structural feature which was not visible in EM of thin sections. In analogy to other retroviruses, the FV MA layer is considered to consist primarily of the N-terminal Gag domain. This assumption is supported by the difference in the sizes of the HFV and FFV MA layers, a difference which likely corresponds to 130 additional residues in the N-terminal region of HFV compared with FFV (Fig. 1D). In contrast, the central and C-terminal Gag domains of the known FV are similar in size (Fig. 1D) (42, 50), corresponding to the almost identical dimensions of FFV and HFV capsids (Table 1). It is assumed that the central and C-terminal regions of FV Gag are

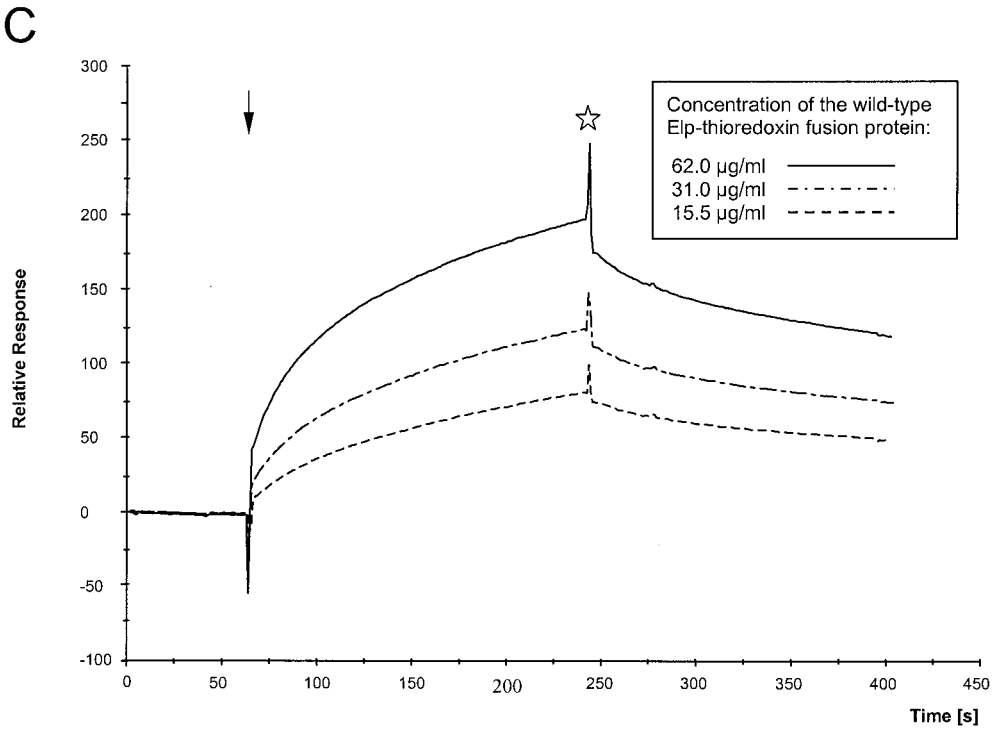

FIG. 8—*Continued.*

primarily involved in capsid formation and genome binding (54). The size and shape of the FV capsid structures do not match those of the hepadnaviruses despite their functional similarities with retroviruses and FV (2).

The second feature that distinguishes FV particles from those of other retroviruses is the fact that the N-terminal domain of the Env precursor Elp, about 16.5 kDa in size, is a virion-associated protein. A similar observation has been previously reported for HFV (D. Lindemann, personal communication), whereas the much smaller N-terminal signal peptides of other retroviruses are not part of the virion (24).

Whereas the function of the classical signal peptide is considered to be the targeting of Env into the lumen of the endoplasmatic reticulum (24), the FV Elp appears to have additional functions. Our present biosensor SPR work reveals a specific interaction of the N-terminal sequences of the Elp with the N-terminal region of the FFV Gag protein in vitro. Two conserved Trp residues in Elp were required for binding. Corresponding interactions have not been shown for any other retrovirus. The data obtained with the substitutions of Ala for Trp in the FFV Elp peptides complement the results of genetic experiments on HFV budding with the same amino acid substitutions (D. Lindemann, personal communication).

The on and off rates and affinities observed in the SPR studies with the Elp peptides and the recombinant N-terminal Elp domain are expected to yield specific and possibly even reversible interactions (25, 41). Virus morphogenesis and the formation of other higher-order protein complexes rely upon concerted effects of many specific interactions. These generate the metastable protein assemblies that support the efficient disassembly that is required for infection (7).

The secondary structure of the Elp peptide is predicted by the computer program DSC for discrimination of protein secondary structure classes (28) to be identical to that in the full-length Env. The part of Elp which had been altered in the mutant peptides is predicted to form a stable helix even when both Trp residues have been replaced with Ala. Due to this intrinsic stability of the secondary structure, the Elp peptides used for the assays may adopt a conformation comparable to that in the viral particle. The significantly stronger binding of Elp residues 1 to 65 in the context of the fusion protein compared to the 30-mer Elp WW peptide indicates that flanking residues and/or the overall folding of the cytoplasmic domain of Elp are important for binding. By analogy, Elp-Gag binding may be further modulated by the conformation and/or processing of the Gag and Env precursor molecules.

Our data indicate that the N-terminal domain of Elp has an intrinsic morphogenetic function in directing specific Env-MA interactions. Such a function would require that the N terminus of Elp be located at the cytoplasmic side of those membranes where FV budding takes place. Consistently, subtilisin digests of purified FFV particles actually showed that the N terminus of Elp is located inside the particle (data not shown). Thus, the direct interaction of FV Elp with Gag may subsume the role played by the membrane binding subdomain of other retrovirus MA proteins. Detailed studies of the HIV-1 MA domain in the context of the Gag precursor have shown that binding of MA to membranes involves at least several domains of the MA protein (17).

The Elp-Gag interaction appears to be unique to FV, since heterologous leader peptides in other retroviruses support the formation of infectious particles. It is conceivable that the

specificity of the FV Elp-Gag interactions is the reason for the inability to pseudotype HFV particles (38). Evidence for Env-Gag interactions has been previously reported for other retroviruses; however, the interactions involve the C-terminally located cytoplasmic tail of Env rather than the leader peptide (17, 35, 44, 51).

Morphological evidence for an Env-Gag interaction was obtained only in the FFV particles with distended morphology (Fig. 3 and Table 2). The morphology of these particles clearly resembled that of the budding forms of other retroviruses including FV (4, 6, 21, 22, 36, 38, 55). The envelope of the distended particles was incompletely closed, and the particles were composed of a spherical portion and a protruding tail (Fig. 3). We interpret them as FFV budding intermediates that coisolated with the properly budded spherical FFV particles. An alternative explanation that they represent disrupted particles or fusion intermediates cannot be ruled out. Nevertheless, the distended forms reveal structural features that may be present transiently during morphogenesis even if these particles are dead-end or abortive assemblies.

Provided that the distended FFV particles represent budding intermediates, the Elp-MA layer interaction could serve the morphogenetic role of targeting preformed FV capsids to the membrane and/or concentrating Env trimers at the site of budding. The FV Elp-MA interaction may interfere with the cytoplasmic Gag targeting and retention of preassembled capsids. Such targeting and retention have been shown to exist for Mason-Pfizer monkey virus Gag and are probably mediated by the interaction of MA sequences with cellular proteins (8). In other retroviruses, membrane targeting and binding are attributed to the MA shell located directly under the viral membrane (17). In FV, lateral Env-Env interactions seen in cEM (Fig. 1 to 3) may provide the driving force that leads to budding of FV particles, explaining the Env dependency of this process in FV (4, 38). After budding is completed, the FV MA layer should need to dissociate from the viral membrane as it remains covalently linked to the capsid. This process may be modulated by proteolysis, which would implicate that the mature Elp may have functions different from those in the uncleaved Env precursor. Additional experiments are required to determine the function of the Elp-Gag interactions during morphogenesis and maturation.

In summary, the combination of cEM, immunoblotting, and SPR allowed us to determine the structural features of FV particles, to identify the virion-associated FFV Elp protein, and to characterize the molecular basis of the FV Gag-Env interactions.

ACKNOWLEDGMENTS

T.W. and V.G. contributed equally to this study.

This study was supported by the Deutsche Forschungsgemeinschaft grants LO 700/1-2 to M.L. and Fu 354/1-1 to S.D.F. and a Wellcome Trust Programme grant to S.D.F. S.D.F. is a Wellcome Trust Principal Research Fellow.

We thank Dirk Lindemann for communicating his results prior to publication. We are grateful to Erika Mancini (EMBL) and Felix deHaas (EMBL) for discussions and help with the CTF correction, Norbert Avemarie (Merck) for help in SPR studies, Helmut Bannert (DKFZ) for excellent technical assistance, and Harald zur Hausen for continuous support.

REFERENCES

1. **Alke, A., A. Schwantes, M. Zemba, R. M. Flügel, and M. Löchelt.** 2000. Characterization of the humoral immune response and virus replication in cats experimentally infected with feline foamy virus. Virology **275:**170–176.
2. **Baker, T. S., N. H. Olson, and S. D. Fuller.** 1999. Adding the third dimension to virus life cycles: three-dimensional reconstruction of icosahedral viruses from cryo-electron micrographs. Microbiol. Mol. Biol. Rev. **63:**862–922.
3. **Baldwin, D. N., and M. L. Linial.** 1999. Proteolytic activity, the carboxy terminus of Gag, and the primer binding site are not required for Pol incorporation into foamy virus particles. J. Virol. **73:**63687–63693.
4. **Baldwin, D. N., and Linial, M. L.** 1998. The roles of Pol and Env in the assembly pathway of human foamy virus. J. Virol. **72:**3658–3665.
5. **Bodem, J., M. Zemba, and R. M. Flügel.** 1998. Nuclear localization of the functional Bel 1 transactivator but not of the gag proteins of the feline foamy virus. Virology **251:**22–27.
6. **Bugelski, P. J., B. E. Maleeff, A. M. Klinkner, J. Ventre, and T. K. Hart.** 1995. Ultrastructural evidence of an interaction between Env and Gag proteins during assembly of HIV type 1. AIDS Res. Hum. Retrovir. **11:**55–64.
7. **Caspar, D. L. D., and A. Klug.** 1962. Physical principles in the construction of regular viruses. Cold Spring Harbor Symp. Quant. Biol. **27:**1–24.
8. **Choi, G., S. Park, B. Choi, S. Hong, J. Lee, E. Hunter, and S. S. Rhee.** 1999. Identification of a cytoplasmic targeting/retention signal in a retroviral Gag polyprotein. J. Virol. **73:**5431–5437.
9. **Coffin, J. M.** 1996. Retroviridae: the viruses and their replication, p. 1767–1847. *In* B. N. Fields, D. M. Knipe, and P. M. Howley (ed.), Virology. Raven Press, New York, N.Y.
10. **Conte, M. R., and S. Matthews.** 1998. Retroviral matrix proteins: a structural perspective. Virology **246:**191–198.
11. **de Haas, F., A. O. Paatero, L. Mindich, D. H. Bamford, and S. D. Fuller.** 1999. A symmetry mismatch at the site of RNA packaging by the polymerase complex of dsRNA bacteriophage phi-6. J. Mol. Biol. **294:**357–372.
12. **Enssle, J., N. Fischer, A. Moebes, B. Mauer, U. Smola, and A. Rethwilm.** 1997. Carboxy-terminal cleavage of the human foamy virus Gag precursor molecule is an essential step in the viral life cycle. J. Virol. **71:**7312–7317.
13. **Erickson, H. P., and A. Klug.** 1971. Measurement and compensation of defocusing and aberrations by Fourier processing of micrographs. Philos. Trans. R. Soc. Lond. B Biol. Sci. **261:**105–118.

13a. **Ferlenghi, I., M. Clarke, T. Ruttan, S. L. Allison, J. Schalich, F. X. Heinz, S. C. Harrison, F. A. Rey, and S. D. Fuller.** 2001. Molecular organization of a recombinant subviral particle from tick-borne encephalitis virus. Mol. Cell **7:**593–602.

14. **Fischer, N., M. Heinkelein, D. Lindemann, J. Enssle, C. Baum, E. Werder, H. Zentgraf, J. G. Muller, and A. Rethwilm.** 1998. Foamy virus particle formation. J. Virol. **72:**1610–1615.
15. **Frank, J., M. Radermacher, P. Penczek, J. Zhu, Y. Li, M. Ladjadj, and A. Leith.** 1996. SPIDER and WEB: processing and visualization of images in 3D electron microscopy and related fields. J. Struct. Biol. **116:**190–199.
16. **Frankel, A. D., and J. A. Young.** 1998. HIV-1: fifteen proteins and an RNA. Annu. Rev. Biochem. **67:**1–25.
17. **Freed, E. O.** 1998. HIV-1 Gag proteins: diverse functions in the virus life cycle. Virology **251:**1–15.
18. **Fuller, S. D., J. A. Berriman, S. J. Butcher, and B. E. Gowen.** 1995. Low pH induces the swivelling of the glycoprotein heterodimers in the Semliki Forest virus spike complex. Cell **81:**715–725.
19. **Fuller, S. D., S. J. Butcher, R. H. Cheng, and T. S. Baker.** 1996. Three-dimensional reconstruction of icosahedral particles: the uncommon line. J. Struct. Biol. **116:**48–65.
20. **Fuller, S. D., T. Wilk, B. E. Gowen, H.-G. Kräusslich, and V. M. Vogt.** 1997. Cryo-electron microscopy reveals ordered domains within the immature HIV-1 particle. Curr. Biol. **7:**729–738.
21. **Gelderblom, H. R.** 1991. Assembly and morphology of HIV: potential effect of structure on viral function. AIDS **5:**617–638.
22. **Gelderblom, H. R., E. H. S. Hausmann, M. Örzel, G. Pauli, and M. A. Koch.** 1987. Fine structure of human immunodeficiency virus (HIV) and immunolocalization of structural proteins. Virology **156:**171–176.
23. **Giron, M. L., S. Colas, J. Wybier, F. Rozain, and R. Emanoil-Ravier.** 1997. Expression and maturation of human foamy virus Gag precursor polypeptides. J. Virol. **71:**1635–1639.
24. **Hunter, E., and R. Swanstrom.** 1990. Retrovirus envelope glycoproteins. Curr. Top. Microbiol. Immunol. **157:**187–253.
25. **Jelonek, M. T., K. Natarajan, and D. H. Margulies.** 2000. Physical measurements of the interaction of MHC molecules and T-cell receptors, p. 115–125. *In* K. Nagata and H. Handa (ed.), Real-time analysis of biomolecular interactions—application of BIACORE. Springer-Verlag, Tokyo, Japan.
26. **Johnsson, B., and G. Malmqvist.** 1992. Real-time biospecific interaction analysis. The integration of surface plasmon resonance detection, general biospecific interface chemistry, and microfluidics into one analytical system, p. 291–336. *In* A. Turner (ed.), Advances in biosensors. JAI Press Ltd., London, United Kingdom.
27. **Johnsson, B., S. Lofas, and G. Lindquist.** 1991. Immobilization of proteins to a carboxymethyldextran-modified gold surface for biospecific interaction

analysis in surface plasmon resonance sensors. Anal. Biochem. **198:**268–277.
28. **King, R. D., M. Saqi, R. Sayle, and M. J. Sternberg.** 1997. DSC: public domain protein secondary structure predication. Comput. Appl. Biosci. **13:** 473–474.
29. **Konvalinka, J., M. Löchelt, H. Zentgraf, R. M. Flügel, and H.-G. Kräusslich.** 1995. Active spumavirus proteinase is essential for virus infectivity but not for formation of the Pol polyprotein. J. Virol. **69:**7264–7268.
30. **Lecellier, C. H., and A. Saib.** 2000. Foamy viruses: between retroviruses and pararetroviruses. Virology **271:**1–8.
31. **Linial, M. L.** 1999. Foamy viruses are unconventional retroviruses. J. Virol. **73:**1747–1755.
32. **Löchelt, M., and R. Flügel.** 1995. The molecular biology of primate spumaviruses, p. 361–397. *In* J. A. Levy (ed.), The Retroviridae, vol. 4. Plenum Press, New York, N.Y.
33. **Löchelt, M., H. Zentgraf, and R. M. Flügel,** 1991. Construction of an infectious DNA clone of the full-length human spumaretrovirus genome and mutagenesis of the bel 1 gene. Virology **184:**43–54.
34. **Morozov, V. A., T. D. Copeland, K. Nagashima, M. A. Gonda, and S. Oroszlan.** 1997. Protein composition and morphology of human foamy virus intracellular cores and extracellular particles. Virology **228:**307–317.
35. **Murakami, T., and E. O. Freed.** 2000. Genetic evidence for an interaction between human immunodeficiency virus type 1 matrix and α-helix 2 of the gp41 cytoplasmic tail. J. Virol. **74:**3548–3554.
36. **Nermut, M. V., and D. J. Hockley.** 1996. Comparative morphology and structural classification of retroviruses. Curr. Top. Microbiol. Immunol. **214:** 1–24.
37. **Pfrepper, K. I., M. Löchelt, H. R. Rackwitz, M. Schnölzer, H. Heid, and R. M. Flügel.** 1999. Molecular characterization of proteolytic processing of the Gag proteins of human spumavirus. J. Virol. **73:**7907–7911.
38. **Pietschmann, T., M. Heinkelein, M. Heldmann, H. Zentgraf, A. Rethwilm, and D. Lindemann.** 1999. Foamy virus capsids require the cognate envelope protein for particle export. J. Virol. **73:**2613–2621.
39. **Rethwilm, A.** 1995. Regulation of foamy virus gene expression. Curr. Top. Microbiol. Immunol. **193:**1–24.
40. **Sakalian, M., and E. Hunter.** 1998. Molecular events in the assembly of retrovirus particles. Adv. Exp. Med. Biol. **440:**329–339.
41. **Slansky, J. E., F. M. Rattis, L. F. Boyd, T. Fahmy, E. M. Jaffee, J. P. Schneck, D. H. Margulies, and D. M. Pardoll.** 2000. Enhanced antigen-specific antitumor immunity with altered peptide ligands that stabilize the MHC-peptide-TCR complex. Immunity **13:**529–538.
42. **Tobaly-Tapiero, J., P. Bittoun, M. Neves, M. C. Guillemin, C. H. Lecellier, F. Puvion-Dutilleul, B. Gicquel, S. Zientara, M. L. Giron, H. de The, and A. Saib.** 2000. Isolation and characterization of an equine foamy virus. J. Virol. **74:**4064–4073.
43. **Turner, B. G., and M. F. Summers.** 1999. Structural biology of HIV. J. Mol. Biol. **285:**1–32.
44. **Vincent, M. J., L. R. Melsen, A. S. Martin, and R. W. Compans.** 1999. Intracellular interaction of simian immunodeficiency virus Gag and Env proteins. J. Virol. **73:**8138–8144.
45. **Vogt, V. M.** 1997. Retroviral virions and genomes, p. 27–70. *In* J. M. Coffin, S. H. Hughes, and H. E. Varmus (ed.), Retroviruses. Cold Spring Harbor Laboratory Press, Cold Spring Harbor, N.Y.
46. **Wilk, T., F. deHaas, A. Wagner, A. Alke, T. Rutten, S. D. Fuller, R. M. Flügel, and M. Löchelt.** 2000. The intact retroviral Env glycoprotein of human foamy virus is a trimer. J. Virol. **74:**2885–2887.
47. **Wilk, T., and S. D. Fuller.** 1999. Towards the structure of the human immunodeficiency virus: divide and conquer. Curr. Opin. Struct. Biol. **9:**231–243.
48. **Wilk, T., B. Gowen, and S. D. Fuller.** 1999. Actin associates with the nucleocapsid domain of the human immunodeficiency virus Gag polyprotein. J. Virol. **73:**1931–1940.
49. **Wilk, T., I. Gross, B. E. Gowen, T. Rutten, F. de Haas, R. Welker, H.-G. Kräusslich, P. Boulanger, and S. D. Fuller.** 2000. The organization of immature HIV-1. J. Virol. **75:**759–771.
50. **Winkler, I., J. Bodem, L. Haas, M. Zemba, H. Delius, R. Flower, R. M. Flügel, and M. Löchelt.** 1997. Characterization of the genome of feline foamy virus and its proteins shows distinct features different from those of primate spumaviruses. J. Virol. **71:**6727–6741.
51. **Wyma, D. J., A. Kotov, and C. Aiken.** 2000. Evidence for a stable interaction of gp41 with $Pr55^{Gag}$ in immature human immunodeficiency virus type 1 particles. J. Virol. **74:**9381–9387.
52. **Yeager, M., E. M. Wilson-Kubalek, S. G. Weiner, P. O. Brown, and A. Rein.** 1998. Supramolecular design of native and immature murine leukemia virus reveals by electron cryo-microscopy. Proc. Natl. Acad. Sci. USA **95:**7299–7304.
53. **Yu, S. F., D. N. Baldwin, S. R. Gwynn, S. Yendapalli, and M. L. Linial.** 1996. Human foamy virus replication: a pathway distinct from that of retroviruses and hepadnaviruses. Science **271:**1579–1582.
54. **Yu, S. F., K. Edelmann, R. K. Strong, A. Moebes, A. Rethwilm, and M. L. Linial.** 1996. The carboxyl terminus of the human foamy virus Gag protein contains separable nucleic acid binding and nuclear transport domains. J. Virol. **70:**8255–8262.
55. **Zemba, M., T. Wilk, T. Rutten, A. Wagner, R. Flügel, and M. Löchelt.** 1998. The carboxy-terminal p3Gag domain of the human foamy virus Gag precursor is required for efficient virus infectivity. Virology **247:**7–13.
56. **Zemba, M., A. Alke, J. Bodem, I. G. Winkler, R. L. P. Flower, K.-I. Pfrepper, H. Delius, R. M. Flügel, and M. Löchelt.** 2000. Construction of infectious feline foamy virus genomes: cat antisera do not cross-neutralize feline foamy virus chimera with serotype-specific Env sequences. Virology **266:**150–156.
57. **Zhou, W., and M. D. Resh.** 1996. Differential membrane binding of the human immunodeficiency virus type 1 matrix protein. J. Virol. **70:**8540–8548.